# Micronuclei Bearing Acentric Extrachromosomal Chromatin Are Transcriptionally Competent and May Perturb the Cancer Cell Phenotype

**Koh-ichi Utani, June-ko Kawamoto, and Noriaki Shimizu**

*Graduate School of Biosphere Science, Hiroshima University, Higashi-hiroshima, Japan*

## Abstract

**Extrachromosomal double minutes (DM) bear amplified genes that contribute to the malignancy of human cancer cells. A novel intracellular behavior of DMs resulted in their selective entrapment within micronuclei; opening the vista, this could perturb the cancer cell phenotype if genes located on DMs were expressed in micronuclei. Here, using fluorescence *in situ* hybridization, we detected transcripts in DM-enriched micronuclei. Visualization of DMs and their transcripts in live cells showed that DMs are as actively transcribed in the micronuclei and nuclei. Moreover, pulse-incorporated bromouridine was detected in the micronuclei, and the transcripts eventually exited from the micronuclei, similar to the behavior of nuclear transcripts. This apparently normal pattern of gene expression in DM-enriched micronuclei was restricted to micronuclei associated with lamin B, and lamin B association was more frequent for micronuclei that incorporated DMs than for those that incorporated a chromosome arm. The frequency of lamin B–associated micronuclei increased after entry into S phase, and accordingly, there was a concomitant increase in transcription in micronuclei. Taken together, these results indicate that the expression of genes on DMs can be temporally altered by their incorporation into micronuclei. This may be relevant for a broad spectrum of other extrachromosomal elements. (Mol Cancer Res 2007;5(7):695–704)**

## Introduction

Gene amplification plays a crucial role in the malignant transformation of human cells as it mediates the activation of oncogenes or the acquisition of drug resistance. Genes that are highly amplified in cancer are localized at extrachromosomal double minutes (DM) or at the chromosomal homogeneously staining region. DMs consist of multiple, paired, minute chromatins of varying sizes and can be detected when the chromosomes are spread out. DMs generally lack the centromere and are composed of circular DNA that does not require a telomeric structure (for a recent review, see refs. 1, 2). We and others have shown previously that the elimination from human tumor cells of the amplified c-*myc* oncogenes on DMs reversed the malignant phenotype of the cells and induced cellular differentiation (3-5). Similar to this finding, elimination of amplified multidrug resistance gene on DMs resulted in reversion to a more drug-sensitive phenotype (6, 7). The elimination of amplified c-*myc* genes was accelerated by the treatment of the cells with low concentration of hydroxyurea (5, 8), and the elimination was accompanied by the specific inclusion of DMs into micronuclei, as shown by fluorescence *in situ* hybridization (FISH) using a DM-specific probe (4, 5). Because the DMs were incorporated into micronuclei in a highly specific manner, the purification of the micronuclei provided highly pure DM DNA (9). We designate these micronuclei in this article as "DM-type micronuclei."

It was generally understood that another class of micronuclei, which we refer to here as "chromosome-type micronuclei," is formed either from acentric chromosomal fragments or from individual chromosomes by clastogenic agents (e.g., γ-irradiation or chemicals that cause DNA double-strand breakage) and aneugenic agents (e.g., spindle poisons), respectively (reviewed in ref. 10). Both types of agents cause genetic materials to be left behind the separating chromosomes during anaphase, which are thought to generate the chromosome-type micronuclei. It has been reported that at least some chromosome-type micronuclei lack a nuclear lamina and are devoid of lamin B protein (a major constituent of the nuclear lamina) and the nuclear pore complex (11-13). On the other hand, generation of DM-type micronuclei depended on the intracellular behavior of DMs during the cell cycle. During mitosis, acentric DMs segregate stably to the daughter cells by tethering to the chromosomes (14-16). Although DMs are composed of early-replicating euchromatin (17), their binding to the mitotic chromosomes leads to their localization in $G_1$ phase at the nuclear periphery, which is rich in heterochromatin. When the DMs themselves replicate during early S phase, they relocate to the nuclear interior (17, 18). Micronucleation of the DMs can be induced by treating DM-containing cells with low concentrations of hydroxyurea at early S phase. When this occurs, the DMs detach from the chromosomes at the next mitosis, aggregate, and are left behind the separating chromosomes at anaphase (16). We have found that, although a significant proportion of

Received 1/22/07; revised 4/3/07; accepted 4/26/07.
**Grant support:** Japan Society for the Promotion of Science Grant-in-Aid for Scientific Research (B) 17370002 (N. Shimizu).
The costs of publication of this article were defrayed in part by the payment of page charges. This article must therefore be hereby marked *advertisement* in accordance with 18 U.S.C. Section 1734 solely to indicate this fact.
**Requests for reprints:** Noriaki Shimizu, Graduate School of Biosphere Science, Hiroshima University, 1-7-1 Kagamiyama, Higashi-hiroshima 739-8521, Japan. Phone: 81-824-24-6528; Fax: 81-824-24-0759. E-mail: shimizu@hiroshima-u.ac.jp

doi:10.1158/1541-7786.MCR-07-0031

these cytoplasmic DMs are not associated with lamin B protein during the subsequent $G_1$ phase, they do seem to be wrapped with lamin B during the next S phase after the synthesis and reorganization of lamin protein (16). Significantly, several viral nuclear plasmids, including bovine papilloma virus (19), Epstein-Barr virus (20), Kaposi's sarcoma–associated herpes virus (21), and SV40 (22), also segregate into daughter cells by tethering to the mitotic chromosomes. Thus, the intracellular behavior of DMs and the process by which they are extracellularly eliminated may be common strategies used by a broad spectrum of autonomously replicating extrachromosomal elements.

It has been proposed repeatedly that the contents of chromosome-type micronuclei may be easily eliminated from the cell (23-25) despite the mechanism was not suggested. Similarly, we showed previously that DM-type micronuclei can be detected in the extracellular culture fluid (26). These extracellular micronuclei were wrapped with both lamin B and cytoplasmic membrane and their DNA had not undergone extensive degradation. Therefore, we proposed that at least some of the cytoplasmic micronuclei may be eliminated from the cell by extrusion. Supporting this is that, when we tracked microinjected DNA in live cells, we observed that the DNA became aggregated in the nucleus and then appeared as

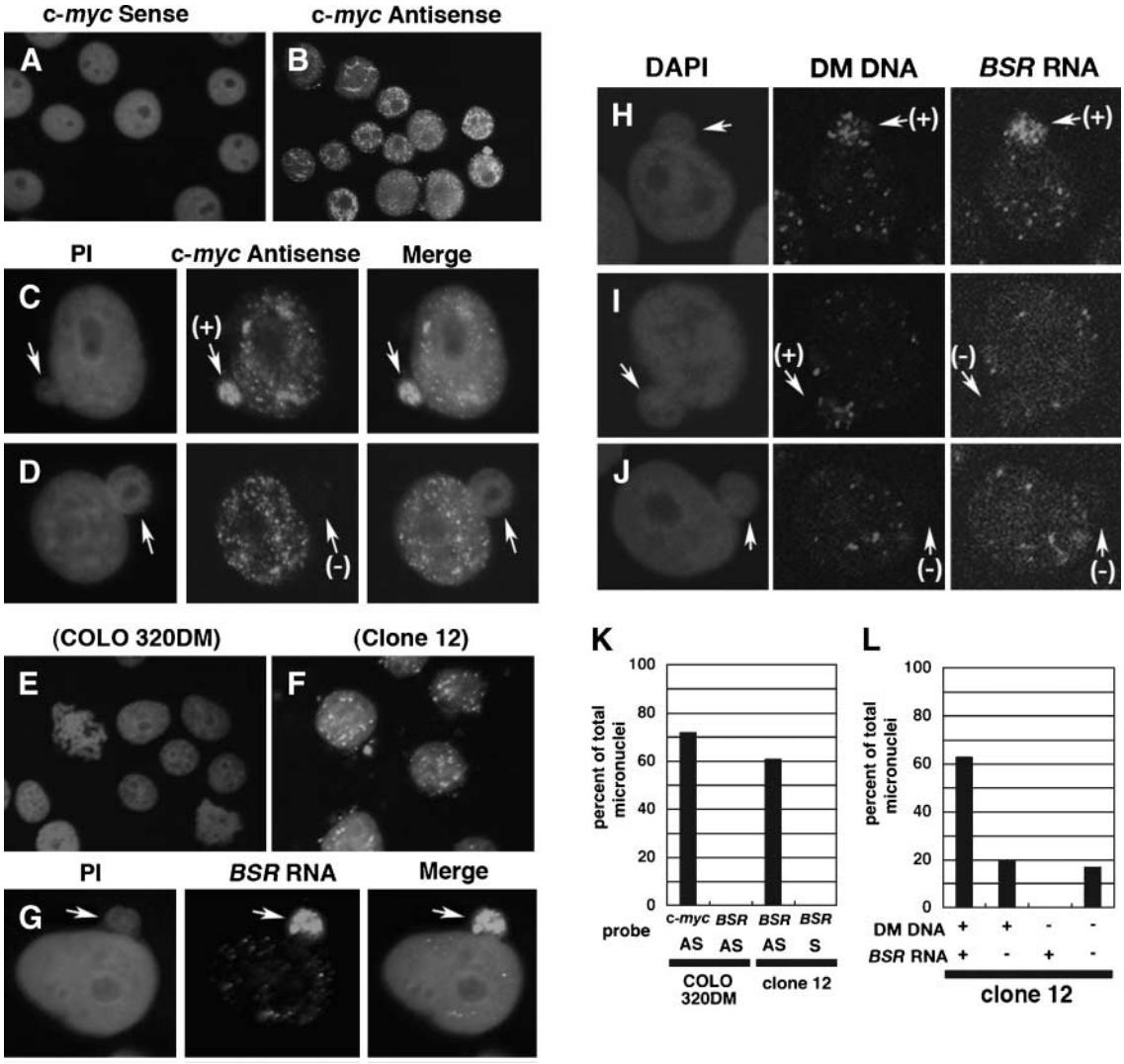


**FIGURE 1.** RNA expressed from DMs was detected in some but not all DM-type micronuclei. Logarithmically growing COLO 320DM cells (**A-E**) or clone 12 cells (**F-J**) were fixed with paraformaldehyde and then hybridized with digoxigenin-labeled c-*myc* sense strand (**A**), c-*myc* antisense strand (**B-D**), or *BSR* antisense strand (**E-J**) RNA probes in nondenaturing conditions. Sequential incubation with a murine anti-digoxigenin antibody and then a FITC-labeled anti-mouse IgG antibody was used to detect the cRNA. In **H** to **J**, *BSR* RNA and DNA were detected simultaneously by first fixing the hybridized RNA signal with paraformaldehyde and then denaturing the slide and hybridizing it with a biotin-labeled plasmid DNA probe. This probe was then visualized by Texas red–conjugated streptavidin. DNA was counterstained by using propidium iodide (*PI*; red, **A-G**) or 4′,6-diamidino-2-phenylindole (*DAPI*; blue, **H-J**). The frequencies of these images were scored and summarized in **K** and **L**. To generate **K**, the indicated probe was hybridized to the indicated cell to detect the cRNA, and the frequencies of the micronuclei showing the hybridized signal relative to the total number of micronuclei (>150) were plotted. AS, antisense; S, sense. To generate **L**, DM DNA and *BSR* RNA was simultaneously detected in clone 12 cells, and the frequencies of the micronuclei showing the indicated signals relative to the total number of micronuclei (>200) were plotted.

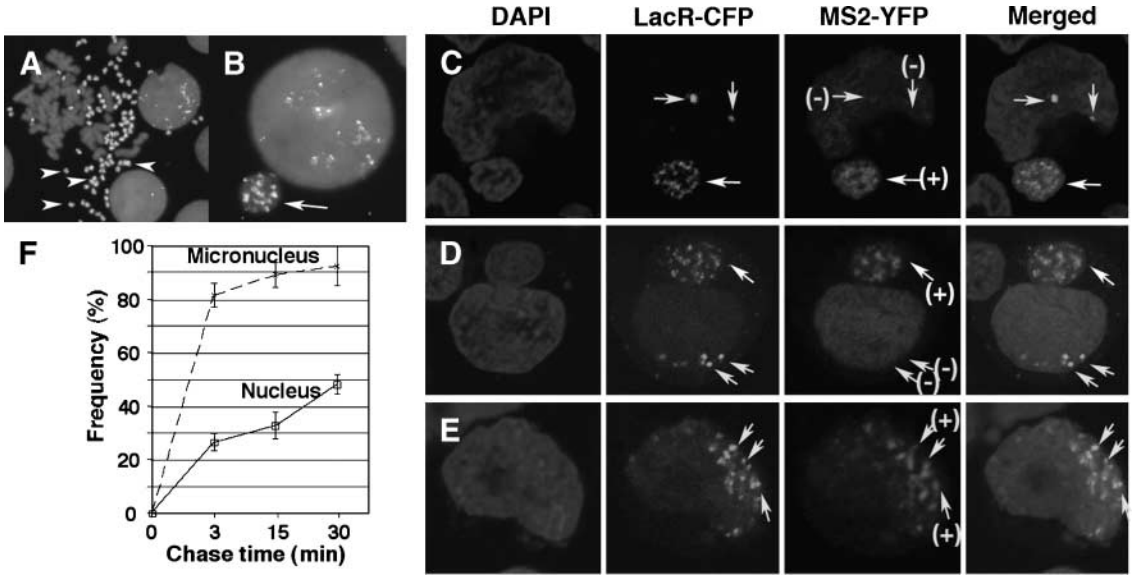


**FIGURE 2.** Visualization of transcription from DMs in live cells. **A** and **B.** Metaphase chromosome prepared from C4C4 cells were hybridized with digoxigenin-labeled pECMS2β DNA and biotin-labeled *DHFR* IR DNA. The hybridized probes were detected by FITC and Texas red, respectively, and DNA was counterstained by 4′,6-diamidino-2-phenylindole (*blue*). **A.** Both pECMS2β and the *DHFR* IR-bearing pΔB.pA plasmid were coamplified at multiple DMs (some of which are indicated by *arrowheads*) among the chromosomes. These DMs were selectively incorporated into the micronuclei (*arrow*) as shown in **B**. **C** to **F.** C4C4 cells were electroporated with a mixture of pMS2-YFP and pTet-ON DNA and, 2.5 h later, incubated with 1 μg/mL doxycycline for 15 min (**C-E**) or the indicated times in the graph (**F**). The cells were fixed with paraformaldehyde and counterstained with 4′,6-diamidino-2-phenylindole. pECMS2β amplified at DMs contains the LacO sequence and can be visualized by the binding of LacR-CFP. pECMS2β transcription can be activated by doxycycline, as doxycycline stimulates the expression of rtTA protein from pTet-ON, which in turns activates the TRE promoter in pECMS2β. The pECMS2β transcripts, which bear the MS2 target sequence, can be visualized by the binding of MS2-YFP protein expressed by pMS2-YFP. The confocal images for 4′,6-diamidino-2-phenylindole, cyan fluorescence protein (*CFP*), and yellow fluorescence protein (*YFP*) were obtained, and these are pseudocolored in blue, green, and red, respectively. **C** to **E.** Representative images. Yellow arrows, DMs in the nucleus; white arrows, DMs in the micronuclei. (+), presence of MS2-YFP near the DMs; (−), absence of MS2-YFP near the DMs. The micronuclei or nuclei in the microscopic field that showed transcription at DMs were scored along with the total micronuclei (30 micronuclei were assessed in each of three independent scoring processes for each time point) or the total nuclei (50 nuclei were assessed in each of three independent scoring processes for each time point), respectively. **F.** The frequencies of the DM-transcribing micronuclei/nuclei were calculated and plotted in the graph.

cytoplasmic micronuclei, which were eventually extruded from the cells (27). However, the timing of extrusion process or the frequency with which it occurs remains unclear. Furthermore, it remains possible that the micronuclear content might be degraded *in situ* in the cytoplasm.

It has been mentioned in a report that chromosome-type micronuclei may be stably maintained in cells for as long as one cell cycle (13). We also observed this when we tracked micronuclei in H2B-green fluorescent protein (GFP) fusion protein-expressing HeLa cells.[1] Thus, micronuclei elimination may occur infrequently and/or require a specific stage of the cell cycle. These observations indicate that micronuclei can persist for quite a long time in the cytoplasm. This in turn suggests that, if the micronuclear genes are expressed and their expression differs from that of the nuclear copy, the presence of micronuclei could significantly perturb the cellular phenotype. That micronuclear genes may be expressed has been suggested by a study that found that purified chromosome-type micronuclei exhibit RNA polymerase activity (28). Another study has revealed that a small proportion of chromosome-type micronuclei show low levels of transcription (13). Whether DM-type micronuclei also show gene expression has not been addressed previously. This is an important issue because DMs carry amplified genes that confer the malignant phenotype; the abnormal expression of these micronuclear genes may thus be responsible, at least in part, for the cancer cell phenotype. Therefore, we here asked whether DM-type micronuclei exhibit gene expression.

## Results and Discussion

### *RNA Transcribed from DMs Was Detected in Some but not All DM-Type Micronuclei*

Previous FISH analysis of logarithmically growing human COLO 320DM cells revealed that ~5% of these cells had DM-type micronuclei and that this frequency was increased to 20% by treatment with a low concentration of hydroxyurea (9, 29). To examine the gene expression activity of DM-type micronuclei in natural conditions in this study, we only examined logarithmically growing cells. The c-*myc* oncogene is amplified at DMs and is overexpressed in COLO 320DM cells. We detected c-*myc* RNA by subjecting the cells to FISH using digoxigenin-labeled c-*myc* RNA probes under nondenaturing conditions. As shown in Fig. 1A and B, the antisense RNA probe, which hybridizes to the sense sequence of the c-*myc* exon 3, hybridized to numerous spots in the cells unlike the sense probe. This is consistent with the observation that the

[1]N. Shimizu et al., unpublished observation.

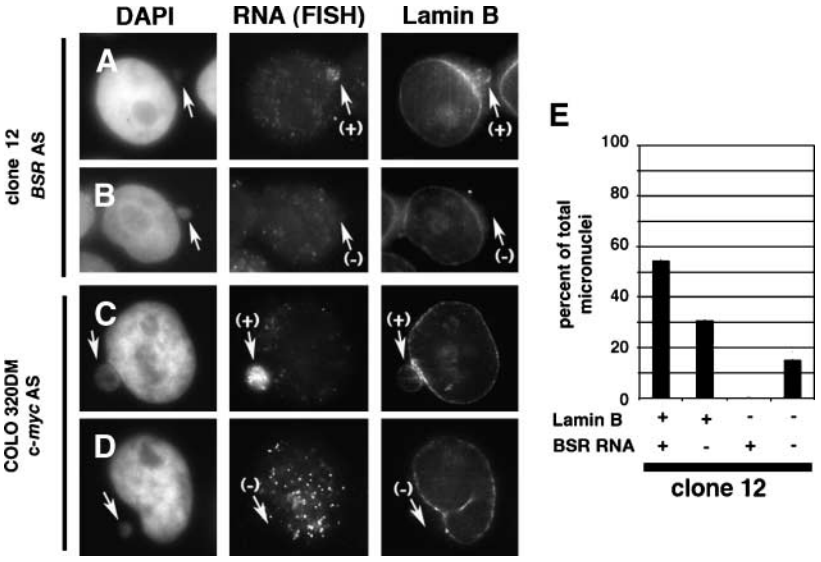


**FIGURE 3.** The association of micronuclei with lamin B is required for their expression of DMs. Clone 12 (**A** and **B**) or COLO 320DM (**C** and **D**) cells were fixed with paraformaldehyde. *BSR* RNA (**A** and **B**) or c-*myc* RNA (**C** and **D**) was detected by FISH using FITC, whereas lamin B was simultaneously detected by immunofluorescence analysis using Texas red (see Materials and Methods for details). Arrows, micronuclei in each epifluorescent image. (+), positive RNA (or lamin B) signals; (−), negative RNA (or lamin B) signals. In **E**, the frequency of each type was calculated (30 micronuclei were assessed in each of three independent scoring processes for each time point) and plotted.

antisense strand of the *c-myc* gene is transcribed because the promoter lies between exons 2 and 3 (30, 31). We found that some but not all micronuclei contained c-*myc* sense strand RNA (Fig. 1C and D). When these two types of micronuclei were counted, it was found the micronuclei with c-*myc* RNA signal comprised ~70% of all the micronuclei in the cell (Fig. 1K).

We previously showed that the gene amplification exhibited by cancer cells can be mimicked by transfecting COLO 320DM cells with pSFVdhfr, a blasticidin resistance (*BSR*)-expressing plasmid that bears an initiation region (IR) and a matrix attachment region (MAR); in the resulting clone 12 cell line, the amplified plasmids reside in multiple preexisting DMs (32). We used FISH with a digoxigenin-labeled *BSR* RNA probe to

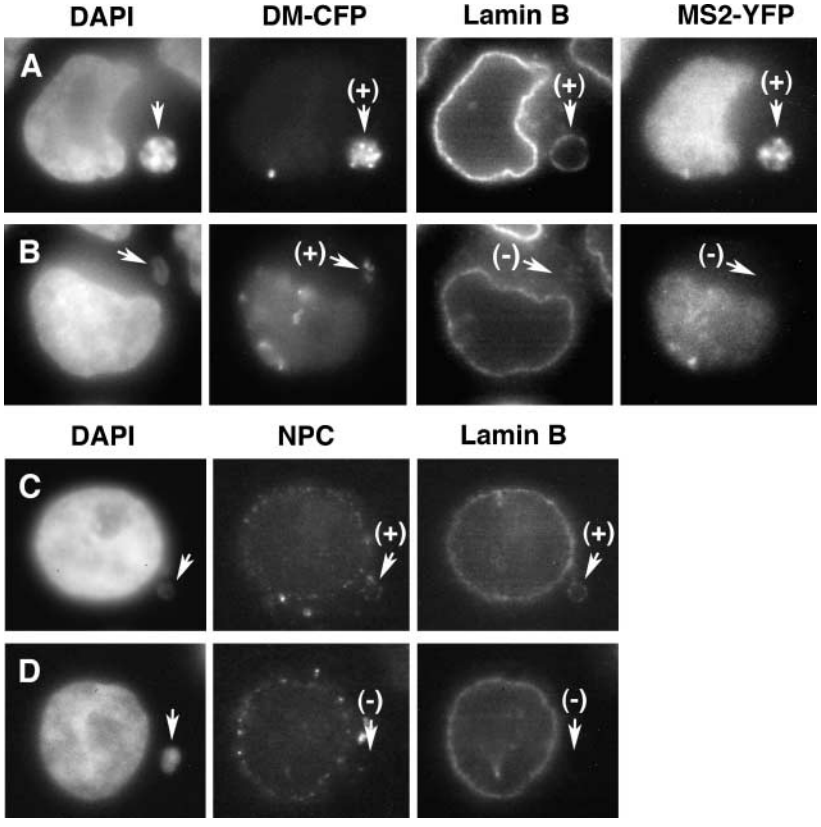


**FIGURE 4.** Micronuclei without lamin B lack a functional nuclear membrane. **A** and **B.** The DMs and their induced transcripts in C4C4 cells were visualized by cyan fluorescence protein and yellow fluorescence protein, respectively, as described in the legend to Fig. 2. The cells were fixed and lamin B was detected by red fluorescence. **A.** Arrow, transcription (yellow fluorescence protein dots) in the DM-CFP–bearing micronuclei was only observed in lamin B–positive micronuclei. **B.** In contrast, the MS2-YFP fusion protein, which bears a nuclear localization signal, did not enter lamin B–negative micronuclei. **C** and **D.** Simultaneous detection of the nuclear pore complex (*NPC*) and lamin B in COLO 320DM cells. Lamin B–positive micronuclei were always nuclear pore complex positive and vice versa.

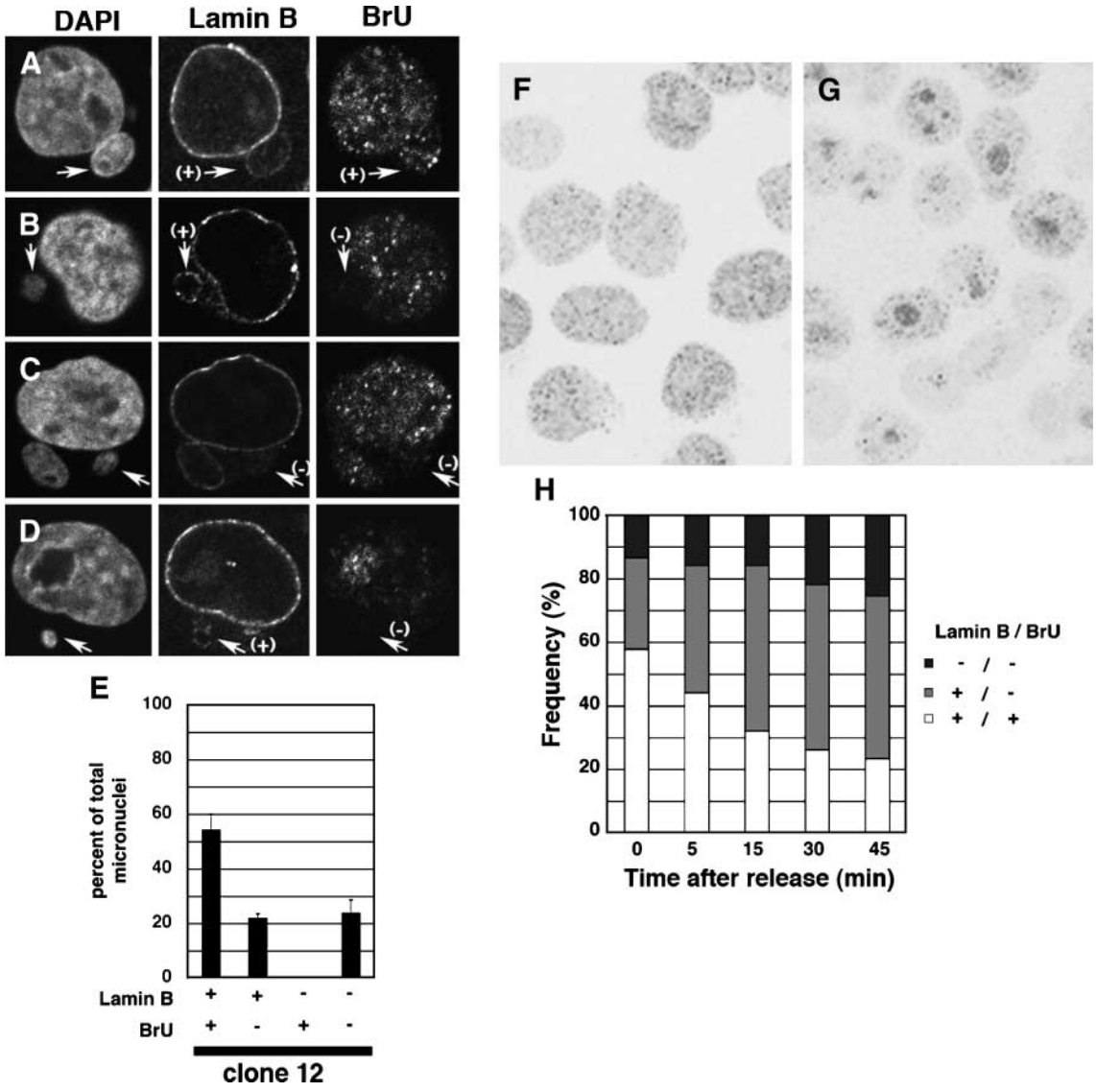


**FIGURE 5.** Bromouridine-labeled nascent transcripts appear in and exit from lamin B–positive micronuclei. Logarithmically growing COLO 320DM cells were pulse labeled with bromouridine (*BrU*), which was then detected along with lamin B. **A** to **C.** Representative images. The frequencies of each pattern were scored (50 micronuclei were assessed in each of three independent scoring processes) and plotted in **E**. The data suggest that association with lamin B is necessary but not sufficient for gene expression in micronuclei. The pulse-labeled cells (**F**) were released in a fresh medium and fixed with paraformaldehyde after 30 min (**D** and **G**) or the times indicated in the graph (**H**). During the release, the nucleoplasmic bromouridine signal disappeared and only the nucleolar signal remained, which suggests the exit of the polymerase II transcripts (**D** and **G**). **H.** The frequencies of the bromouridine-labeling and lamin B–labeling patterns in >100 cells that were assessed were plotted in the graph. The data suggest that the RNA transcribed in the micronuclei might exit to the cytoplasm as does the nuclear-transcribed RNAs.

determine whether the micronuclei express *BSR* RNA. No signal was detected in the parental COLO 320DM cells (Fig. 1E and K), which showed that the background signal was negligible. In contrast, the same probe produced bright signals in clone 12 cells (Fig. 1F) that were concentrated in some but not all of the micronuclei (Fig. 1G and K). About 60% of all micronuclei had concentrated *BSR* RNA, similar to the frequency of the c-*myc* RNA-positive micronuclei in the COLO 320DM cells (Fig. 1K).

COLO 320DM cells have both DM-type and chromosome-type micronuclei, which can appear in single cells as distinct entities. Above experiments did not discriminate between these two types. Therefore, we modified the FISH protocol so that we could simultaneously detect *BSR* RNA and the plasmid sequence on the DM DNA of clone 12 cells. Representative images are shown in Fig. 1H to J, and the frequency of each pattern is shown in Fig. 1L. Micronuclei that only had *BSR* RNA and no DM DNA were not detected, which shows that the background was negligible. The DM DNA–positive micronuclei comprised 82% of all micronuclei. Of these, 72% (62% of all micronuclei) contained a concentrated *BSR* RNA signal. During the course of this study, we did at least three independent experiments, and the data were at least qualitatively reproducible. These data suggest that DMs may be

transcribed in micronuclei. However, because it remained possible that nuclear-transcribed RNA may subsequently concentrate specifically in micronuclei, we did the following experiments.

*Visualization of Transcription from the DMs Inside Micronuclei in Live Cells*

To determine whether the DMs in the micronuclei are actually transcribed, we developed the C4C4 cell line, which allowed us to simultaneously visualize both the DM DNA and its induced transcript RNA in live cells. As described in Materials and Methods, the cell line was generated from COLO 320DM cells by transfection with five plasmids (i.e., pECMS2β,pΔB.pA, pSV2 ECFP-LacR, pTet-ON, and pMS2-YFP). The focal plasmid here is pECMS2β (33). This plasmid was amplified in the host cells due to cotransfection with pΔB.pA, which bears a *DHFR* IR and a MAR (32). This was verified by FISH analysis, which showed that both the IR/MAR plasmid and pECMS2β sequences were coamplified at DMs in these cells (Fig. 2A) and that the DMs were specifically trapped in the micronuclei (Fig. 2B). To visualize the pECMS2β DNA, we took advantage of the fact that it bears *LacO* repeat sequences that can be bound by the LacR-CFP protein (which is expressed by pSV2 ECFP-LacR). To induce transcription from pECMS2β, we took advantage of the fact that pECMS2β bears a TRE promoter that can be activated by the rtTA protein from pTet-ON, whose expression is induced by the addition of doxycycline. To visualize the doxycycline-induced pECMS2β transcripts, we used the fact that these transcripts bear the MS2 target sequence, which can be visualized by the binding of MS2-YFP protein, which is expressed by pMS2-YFP. When we incubated C4C4 cells in the presence of doxycycline, we clearly detected *de novo* transcription from the DMs inside the micronuclei (Fig. 2C and D). The induction was rapid as MS2-YFP was already observed in 80% of the DM-enriched micronuclei within 3 min of adding doxycycline; at 30 min, transcription was observed in ~100% of the pECMS2β DMs. That nearly all micronuclei with pECMS2β DMs were transcribed differs from our observations summarized in Fig. 1L, which shows that only 72% of the micronuclei with pSFVdhfr DMs showed specific transcription. This point will be discussed later. pECMS2β DM transcription was also detected inside the nucleus and the resulting transcripts tended to be concentrated near these nuclear pECMS2β DMs. However, unlike the pECMS2β DMs in the micronuclei, the nuclear transcripts were induced much more slowly, as only half of the nuclei showed pECMS2β DM transcription 30 min after induction. This suggests that the DM transcriptional activity in the micronuclei is higher than in the nucleus. Alternatively, it might simply reflect that the DMs occur at a much higher density in the micronuclei and that the transcription from DMs scattered throughout the nucleus might be more difficult to detect by the method we used.

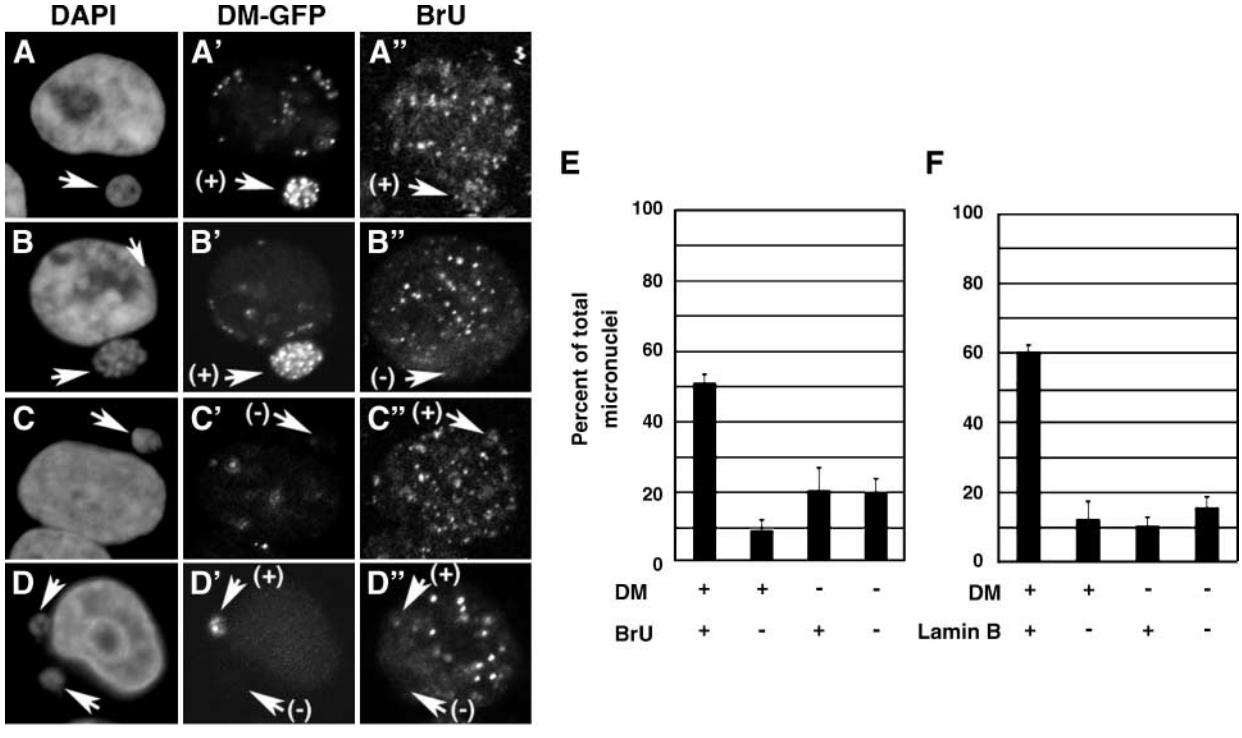


**FIGURE 6.** DM-type micronuclei associate with lamin B and show gene expression more frequently than chromosome-type micronuclei. The DMs in the COLO 320–derived 3B5 cell line were visualized by GFP as described in Materials and Methods. Pulse-incorporated bromouridine was detected in these cells by red fluorescence. **A** to **D.** Representative images. **E.** The frequencies of these patterns were scored and plotted by assessing >50 micronuclei in each of three independent scoring processes at each time point. The data show that most of the DM-type micronuclei, but only half of the DM-negative chromosome-type micronuclei, were bromouridine positive. The frequency of lamin B detection in these cells was plotted in **F**. The data show that the DM-type micronuclei were more frequently associated with lamin B at frequencies resembling those in **E**.

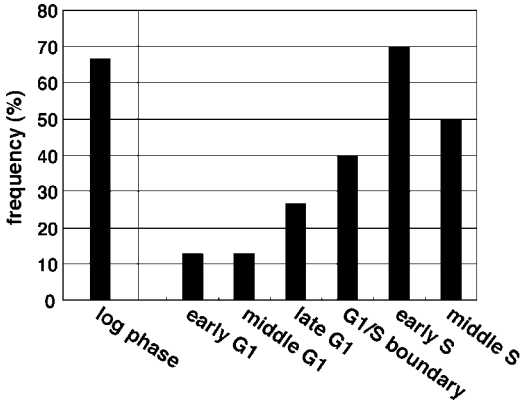


**FIGURE 7.** Gene expression in the micronuclei varies as the cell cycle progresses. The frequencies of c-*myc* DNA-bearing micronuclei that also contain c-*myc* RNA were scored. c-*myc* DNA and RNA were simultaneously detected in logarithmically growing COLO 320DM cultures or the cultures synchronized by the two methods described in Materials and Methods. The early, middle, and late $G_1$ phases correspond to 3, 6, and 9 h after release from nocodazole block, respectively, whereas the $G_1$-S boundary and early and middle S phases correspond to 0, 2, and 6 h after release from aphidicolin block, respectively.

### *Normal Lamina Is Required but not Sufficient for Transcription in the Micronuclei*

The data in Fig. 1 revealed that some but not all micronuclei show transcription. As described in Introduction, some of the chromosome-type micronuclei lack nuclear lamina (11-13). Furthermore, we reported previously that the association of DM-type micronuclei with lamin B changes during progression through the cell cycle (16). Therefore, we examined the possibility that the transcriptional heterogeneity of the micronuclei might reflect variable association with lamina. To test this, we simultaneously detected lamin B and *BSR* RNA in clone 12 cells by immunofluorescence and RNA FISH, respectively. Representative images are shown in Fig. 3 along with a graph summarizing the frequency of the various expression patterns. About 15% of all micronuclei did not associate with lamin B, and all of these were devoid of *BSR* RNA. In contrast, of the remaining 85% of micronuclei, which were all lamin B positive, 65% had *BSR* RNA. That *BSR* RNA was always associated with the presence of lamin is consistent with the notion that lamin B is required for transcription in micronuclei. When similar experiments were done with COLO 320DM cells, c-*myc* RNA was also only detected in the lamin B–positive micronuclei (see Fig. 3C and D for representative images).

We then assessed the colocalization of lamin B with the pECMS2β-expressing micronuclei in C4C4 cells (Fig. 4A and B). All micronuclei that expressed pECMS2β, as detected by spots of MS2-YFP, were rimmed with lamin B (Fig. 4A). In the few cases where the micronuclei were not encircled by lamin B, MS2-YFP protein was also not detected (Fig. 4D). Thus, it seems that lamin B is required for the entrance into micronuclei of nuclear localization signal-bearing proteins, such as MS2-YFP. Furthermore, if we simultaneously detected lamin B and the nuclear pore complex component, both signals always appeared at the micronuclei concurrently (Fig. 4C and D). Therefore, the presence of lamin B at DM-type micronuclei suggests that they bear a normal lamina structure.

To obtain further evidence that lamin B may be required for DM gene transcription in micronuclei, we assessed whether recently occurring transcription from micronuclei bearing pECMS2β DMs is only detected when the micronuclei are associated with lamin B. For this, COLO 320DM cells were pulse treated with bromouridine. Representative images in which bromouridine and lamin B are simultaneously detected are shown in Fig. 5A to D, and the frequencies of each expression pattern are summarized in Fig. 5E. All of the lamin B–negative micronuclei lacked the bromouridine signal, which suggests again that lamin B is required for micronuclear transcription. However, of the 76% of lamin B–positive micronuclei, 22% lacked the bromouridine signal. Thus, the presence of lamin B is necessary but not sufficient for micronuclear transcription. Another factor, such as the cell cycle position, may also be needed for transcription in the micronuclei. This brings us back to the observation that ~100% of the micronuclei in C4C4 cells showed transcriptional activation (Fig. 2F). In this experiment, we only counted the micronuclei that incorporated MS2-YFP, and these should be the lamin B–positive micronuclei. It is possible that the TRE promoter in pECMS2β is so strongly induced by the VP16 acidic activation domain of the rtTA protein that it forces the transcription of the *pECMS2β* gene in all lamin B–positive micronuclei irrespective of their status with regard to the unknown other factor(s) described above.

### *The Transcripts May Exit from the Micronuclei as They Do from the Nuclei*

To determine the behavior of the transcripts over time, after bromouridine pulse labeling of COLO 320DM cells, we released the cells in fresh medium, harvested them after varying chase times, and simultaneously detected lamin B and bromouridine. The bromouridine signal was initially scattered throughout the nucleus (Fig. 5F) but this disappeared by 30 min of chase, leaving only a nucleolar signal (Fig. 5G). This should reflect the exit of nascent transcripts from the nucleus to the cytoplasm for translation, whereas newly transcribed rRNA remained at the nucleolus. During this period, we found that the frequency of bromouridine-negative micronuclei increased, whereas the bromouridine-positive micronuclei decreased. A typical image after the chase time is shown in Fig. 5D, and the frequencies of each pattern are summarized in Fig. 5H. This suggests that the transcripts exit from the micronuclei similar to the behavior of transcripts in the nucleus.

### *DM-Type Micronuclei Associate with Lamin B and Express DM Genes More Frequently than Chromosome-Type Micronuclei*

To visualize the DMs by GFP, we developed the 3B5 COLO 320DM subclone as described in Materials and Methods. These cells allowed us to detect the DMs without the DNA denaturation needed in the FISH procedure. We used these cells to simultaneously detect DMs and the pulse-incorporated bromouridine. Representative images are shown in Fig. 6A to D, and the frequencies of the different patterns are shown in Fig. 6E. About 60% of all micronuclei were of the DM-type, whereas the remaining 40% were of the chromosome-type. As

expected, there were both bromouridine-positive and bromouridine-negative micronuclei. However, unexpectedly, whereas ~83% (50%/60%) of the DM-type micronuclei were bromouridine positive, only half of the chromosome-type micronuclei were bromouridine positive. This suggests that transcription occurs more frequently in the DM-type micronuclei than in the chromosome-type micronuclei. Furthermore, detection of lamin B protein in these cells revealed that 86% (60%/70%) of the DM-type micronuclei were associated with lamin B, whereas almost half of the chromosome-type micronuclei lacked lamin B. These frequencies closely match the bromouridine-positive frequencies, which suggests that DM-type micronuclei associate more frequently with lamin and thus are more prone to be transcribed than chromosome-type micronuclei.

### *The Expression of DM in Micronuclei Changes during Cell Cycle Progression*

Up to this point, we have shown that the gene expression of DMs in micronuclei depends on their lamin B association. Significantly, we have also previously observed that lamin B–positive micronuclei increase in frequency after the S phase (16). This suggests that gene expression in micronuclei may change during the cell cycle progression. To address this issue, we synchronized the COLO 320DM cells, harvested them at various stages of the cell cycle, and simultaneously detected c-*myc* RNA and DNA. The frequencies of c-*myc* DNA-bearing micronuclei that also contained c-*myc* RNA were determined. As summarized in Fig. 7, these frequencies increased dramatically in cultures enriched with early S-phase cells. This is consistent with our observation that lamin associates with micronuclei during early S-phase (16). Thus, the kinetics of DM gene expression in micronuclei seems to be determined by their association with lamin. This suggests that the mechanisms regulating the expression of DM genes may differ markedly from the mechanisms that control the expression of the gene in the nucleus. An example of this is that, although c-*myc* is expressed throughout the cell cycle in normal cells (34), the same gene in DM-type micronuclei is only expressed during S phase.

### *Implications of This Study*

We have shown here that the genes on DMs can be expressed in micronuclei and that this expression is dependent on the association of micronuclei with lamin as well as other, as yet uncharacterized, conditions. That DM genes are expressed in micronuclei is supported by (*a*) the detection of specific RNA transcripts in micronuclei by FISH, (*b*) the visualization of specific transcription in micronuclei in live cells, and (*c*) the detection of pulse-incorporated bromouridine in micronuclei. We also found that the transcripts may then exit from the micronuclei similar to the behavior of nuclear transcripts. That transcription in micronuclei depends on the association with lamin B is suggested by our observation that DM gene expression only occurred in lamin-rimmed micronuclei. This notion is further supported by our observation that the lamin B–negative micronuclei were also devoid of nuclear pore complex and proteins bearing a nuclear localization signal. We believe that this dependency on lamin association restricts the gene expression in micronuclei to a specific stage of the cell cycle (i.e., after entry into S phase). This may have a profound effect on cancer cell phenotype as suggested by the example of the c-*myc* oncogene. It has been reported that, in normal cells, the c-*myc* oncogene is expressed throughout the cell cycle in normal cells (34). In cancer cells, this situation is distorted by the amplification of c-*myc*, which results in c-myc protein overproduction that can contribute to the malignant transformation of, for example, COLO 320DM cells. Our observations suggest that this situation may be even more distorted than previously understood because the expression of the amplified c-*myc* oncogenes is concentrated at a particular time point of the cell cycle rather than occurring throughout the cell cycle.

We also found that DM-type micronuclei were more frequently associated with lamin B than the chromosome-type and that this seemed to enhance the expression potential of the DM-type micronuclei. Future studies will be needed to explain this disparity between the two types of micronuclei. Nevertheless, our observations suggest that expression in DM-type micronuclei may influence the cell phenotype more profoundly than expression in chromosome-type micronuclei.

As described in Introduction, many viral nuclear plasmids act like micronuclei in that they segregate to the daughter cells by sticking to the mitotic chromosome. Thus, it seems that a broad spectrum of autonomously replicating genetic material in mammalian cells uses this mechanism. The detachment of these materials from the chromosome releases them into the cytoplasm after the end of mitosis (35), which may form the micronucleus at the following interphase as in the case of DMs. We had also shown that the DNA microinjected in the nucleus appeared as cytoplasmic micronucleus after cell division (27). Thus, transcription in the micronucleus may have important implications not only for DMs that affect the cancer phenotype but also for the viral pathogenesis or any other phenotype change that is caused by extrachromosomal elements, such as artificially introduced genes.

## Materials and Methods

### *Cell Lines and Culture*

Human COLO 320DM (CCL 220) neuroendocrine tumor cells were obtained and maintained as described previously (9). There are on average ~64 copies of the c-*myc* oncogene in these cells, which are localized to DMs. The "clone 12" cell line we developed has been described previously (36). This line was generated on the basis that plasmids bearing an IR and a MAR are quite efficiently amplified in human cancer cells (32). Thus, clone 12 was obtained by transfection of COLO 320DM cells with a pSFVdhfr plasmid that bears a replication IR and a MAR from the *DHFR* locus; stable transformants were selected by blasticidin. We showed that the introduced plasmid in clone 12 was amplified and localized in DMs. For the current study, we established the C4C4 cell line from COLO 320DM. The DMs in this line can be visualized by their cyan fluorescence and the inducible transcription from the DMs is indicated by yellow fluorescence. This line was obtained by combining the IR/MAR plasmid–based method, which allows us to amplify a desired sequence on DMs (32, 36), with a method to visualize specific DNA and its RNA transcripts in live cells (33), as follows. We first transfected COLO 320DM with the pSV2 ECFP-LacR

plasmid (a generous gift from Dr. Susan M. Janicki and Dr. David L. Spector, Cold Spring Harbor Laboratory, Cold Spring Harbor, NY), which expresses a fusion protein composed of lactose repressor and enhanced cyan fluorescence protein. We isolated a stable clone where the cyan fluorescence was uniformly detected throughout the nucleus. To such cells, we cotransfected pΔB.pA plasmid (36) that bears a *DHFR* IR and MAR and pECMS2β plasmid (a generous gift from Drs. Janicki and Spector). From such transfection, we obtained a clone where both the plasmid sequences were coamplified at multiple DMs, which was confirmed by the dual-color FISH using the probes specific to *DHFR* IR and to *LacO* repeat (see Results). These DMs were visible as small cyan dots by the binding of LacR-CFP to the *LacO* repeat in pECMS2β sequence. To these cells, we electroporated this clone with the pTet-ON (Clontech Laboratories, Inc.) and pMS2-YFP (a generous gift from Drs. Janicki and Spector) plasmids by using a Bio-Rad Gene Pulser at 960 μF, 200 mV. The pECMS2βplasmid bears a TRE promoter that is induced by the rtTA protein, which is expressed from pTet-ON in the presence of doxycycline. The RNA transcribed from the TRE promoter has an MS2 target sequence that can be visualized by the binding of MS2-YFP protein, which is expressed by pMS2-YFP.

We also established the 3B5 cell line, in which the DMs are visualized by their expression of GFP, by using a previously described procedure used to visualize homogeneously staining region (37). Briefly, COLO 320DM cells that already expressed the LacR-GFP fusion protein (36) were cotransfected with a plasmid bearing a c-*myc* IR and an Igκ MAR (pNeo.Myc ΔSVAR) and a plasmid bearing *LacO* (pSV2-dhfr 8.32). The transformants were selected in the presence of 400 μg/mL G418, and clones exhibiting multiple small nuclear GFP foci were identified under a fluorescence microscope. We confirmed that the plasmid sequences were actually amplified at the DMs by FISH using a probe specific for the LacO sequence (data not shown). All the transfections were done by using the Gene Porter 2 lipofection kit (Genlantis Co.), unless otherwise indicated. COLO 320DM and all its derivative cell lines were cultured in RPMI 1640 supplemented with 10% FCS.

Cell cycle synchronization was done according to our published protocol developed for COLO 320DM cells (16). Briefly, COLO 320DM cells were arrested at S phase by treatment with 2 mmol/L thymidine for 17 h, released for 12 h in fresh medium containing 25 μmol/L deoxycytidine, and again arrested at the $G_1$-S boundary by treatment with 2 μg/mL aphidicolin for 17 h. After release from the $G_1$-S boundary, the S-phase cells were harvested. Alternatively, the cells arrested at the $G_1$-S boundary were released in fresh medium for 9 h and then cultured for an additional 13 h in the presence of nocodazole at a final concentration of 0.4 μg/mL. The cells, which were arrested at prometaphase, were then released into the $G_1$ phase and harvested.

### *Fluorescence* In situ *Hybridization*

The c-*myc* genomic clone in the *Cla*I-*Eco*RI fragment that encompasses exon 3 was recloned into the pGEM4 plasmid vector. A 395-bp fragment encompassing the *BSR* gene was amplified by PCR and also cloned into the pGEM4 vector. The primer sequence used will be provided on request. To prepare the antisense and sense RNA probes, the DNAs of the pGEM4 plasmids containing c-*myc* or *BSR* were linearized by an appropriate restriction enzyme and then transcribed by using SP6-RNA or T7-RNA polymerase and digoxigenin-dUTP or biotin-dUTP. To detect the DNA by FISH, c-*myc* cosmid DNA (9) or pSFVdhfr plasmid DNA was labeled as described previously (32) and hybridized in denaturing conditions to COLO 320DM or clone 12 cells, respectively.

The cells were fixed for the FISH detection of RNA and DNA inside the nuclei or micronuclei as follows. The cells were washed once with PBS without divalent cations ($PBS^-$), cytocentrifuged on poly-L-lysine–coated glass slides (Matsunami Glass Industry Ltd.), and then treated with prechilled CSK buffer [100 mmol/L NaCl, 300 mmol/L sucrose, 10 mmol/L PIPES (pH 6.8), 3 mmol/L $MgCl_2$, 1 mmol/L EGTA, 0.5% Triton X-100, 1.2 mmol/L phenylmethylsulfonyl fluoride, 1.2 mmol/L vanadyl adenosine] for 30 s on ice. The solution was replaced with 4% paraformaldehyde in $PBS^-$ and the cells were fixed for 15 min at room temperature. The slides were then washed with $PBS^-$ and stored in 70% ethanol at 4°C.

To detect specific RNA (RNA FISH), cells on slides were washed once with $PBS^-$ and treated with equilibration solution (50% formamide, 2× SSC) for 15 min at room temperature. The hybridization mixture, which consisted of 20 to 40 ng digoxigenin-labeled probe, 10 μg salmon sperm DNA, 50% formamide, 10% dextransulfate, and 2× SSC in 15 μL for each slide, was denatured at 75°C for 5 min and then applied onto the nondenatured slide. The slide was covered and hybridization was allowed to occur overnight at 37°C. Stringent washing and detection of the hybridized digoxigenin-labeled probe by using an anti-digoxigenin mouse monoclonal antibody (Roche Diagnostics Co.) and a FITC-labeled donkey anti-mouse IgG antibody (Rockland Co.) were done as described previously (16, 17). To simultaneously detect RNA and DNA, specific RNA was detected as above and then the signal was fixed by 3% paraformaldehyde in $PBS^-$ for 10 min at room temperature. The slides were washed with $PBS^-$ and further fixed by immersion in methanol/acetic acid (3:1) for 10 min at room temperature. Slide denaturation and hybridization with a denatured biotin-labeled DNA probe were done as described previously (16), and visualization of the probe was mediated by the use of Texas red–conjugated streptavidin (Invitrogen Co.) and a biotinylated goat anti-streptavidin antibody (Vector Co.).

### *Other Cytochemical Procedures*

Bromouridine (Sigma Co.) was added to the culture at a final concentration of 2.5 mmol/L, and the cells were cultured for 15 min under normal conditions. The cells were washed with $PBS^-$ and fixed with 1.75% paraformaldehyde in $PBS^-$ for 10 min at room temperature. The slide was washed, permeabilized with 0.5% NP40 for 10 min, and blocked by using the Signal Enhancer (Molecular Probes Co.). The incorporated bromouridine was detected by a mouse monoclonal anti-bromodeoxyuridine antibody (Roche Diagnostics) and a FITC-conjugated donkey anti-mouse IgG antibody (Rockland). Lamin B was detected by using a goat anti-lamin B1 (C-20) antibody (Santa Cruz Biotechnology, Inc.) and a Texas red–conjugated anti-goat IgG antibody (EY Laboratories, Inc.).

*Image Acquisition and Processing*

Images were obtained by using either of the following three microscopes. For the images in Fig. 1A to G, a Bio-Rad MRC600 confocal system on a Zeiss Axiovert 135 microscope equipped with a 63× objective (Apochromat, 1.40 numerical aperture, oil) or a 100× objective (Plan-Neofluor, 1.30 numerical aperture, oil) was used. For the images in Figs. 1H to J, 2C to E, and 5A, B, C, D, F, and G, a Zeiss confocal system LSM5 Pascal on a Axiovert 200M equipped with a 63× objective was used. For the images in Figs. 2A and B, 3A to D, 4A to D, and 6A to D, an epifluorescence microscope (Eclipse TE2000-U, Nikon) equipped with a 100× objective lens (Nikon Plan Fluor, 1.30 numerical aperture, oil) was used. In this case, digital images were acquired with a Fuji FinePix S1 Pro digital camera (Fuji Film Co.) or a Leica DFC340 FX camera. All of the acquired digital images were expressed as pseudocolors and merged by using Adobe Photoshop CS version 8.0.1 (Adobe Systems, Inc.).

## Acknowledgments

We thank Dr. Susan M. Janicki and Dr. David L. Spector for their kind gift of pECMS2b, pLacR-CFP, and pMS2-YFP. This work was carried out by using a confocal microscopy at the Analysis Center of Life Science, Hiroshima University.

## References

1. Albertson DG. Gene amplification in cancer. Trends Genet 2006;22:447–55.

2. Myllykangas S, Knuutila S. Manifestation, mechanisms and mysteries of gene amplifications. Cancer Lett 2006;232:79–89.

3. Shimizu N, Nakamura H, Kadota T, et al. Loss of amplified c-myc genes in the spontaneously differentiated HL-60 cells. Cancer Res 1994;54:3561–7.

4. Eckhardt SG, Dai A, Davidson KK, Forseth BJ, Wahl GM, Von Hoff DD. Induction of differentiation in HL60 cells by the reduction of extrachromosomally amplified c-myc. Proc Natl Acad Sci U S A 1994;91:6674–8.

5. Von Hoff DD, McGill JR, Forseth BJ, et al. Elimination of extrachromosomally amplified MYC genes from human tumor cells reduces their tumorigenicity. Proc Natl Acad Sci U S A 1992;89:8165–9.

6. Sanchez AM, Barrett JT, Schoenlein PV. Fractionated ionizing radiation accelerates loss of amplified MDR1 genes harbored by extrachromosomal DNA in tumor cells. Cancer Res 1998;58:3845–54.

7. Schoenlein PV, Barrett JT, Kulharya A, et al. Radiation therapy depletes extrachromosomally amplified drug resistance genes and oncogenes from tumor cells via micronuclear capture of episomes and double minute chromosomes. Int J Radiat Oncol Biol Phys 2003;55:1051–65.

8. Von Hoff D, Forseth B, Bradley T, Wahl G. Hydroxyurea can decrease oncogene copy number in human tumor cell lines. Proc Am Soc Clin Oncol 1990;9:55.

9. Shimizu N, Kanda T, Wahl GM. Selective capture of acentric fragments by micronuclei provides a rapid method for purifying extrachromosomally amplified DNA. Nat Genet 1996;12:65–71.

10. Fenech M. The *in vitro* micronucleus technique. Mutat Res 2000;455:81–95.

11. Willingale TJ, Schweiger M, Hirsch KM, Meek AE, Paulin LM, Traub P. Ultrastructure of Fanconi anemia fibroblasts. J Cell Sci 1989;93 (Pt 4):651–65.

12. Paulin LM, Blake DL, Julien M, Rouleau L. The MAN antigens are non-lamin constituents of the nuclear lamina in vertebrate cells. Chromosoma 1996; 104:367–79.

13. Hoffelder DR, Luo L, Burke NA, Watkins SC, Gollin SM, Saunders WS. Resolution of anaphase bridges in cancer cells. Chromosoma 2004;112:389–97.

14. Kanda T, Wahl GM. The dynamics of acentric chromosomes in cancer cells revealed by GFP-based chromosome labeling strategies. J Cell Biochem 2000; Suppl:107–14.

15. Levan A, Levan G. Have double minutes functioning centromeres? Hereditas 1978;88:81–92.

16. Tanaka T, Shimizu N. Induced detachment of acentric chromatin from mitotic chromosomes leads to their cytoplasmic localization at $G_1$ and the micronucleation by lamin reorganization at S phase. J Cell Sci 2000;113:697–707.

17. Shimizu N, Ochi T, Itonaga K. Replication timing of amplified genetic regions relates to intranuclear localization but not to genetic activity or G/R band. Exp Cell Res 2001;268:201–10.

18. Itoh N, Shimizu N. DNA replication-dependent intranuclear relocation of double minute chromatin. J Cell Sci 1998;111:3275–85.

19. Lehman CW, Botchan MR. Segregation of viral plasmids depends on tethering to chromosomes and is regulated by phosphorylation. Proc Natl Acad Sci U S A 1998;95:4338–43.

20. Marechal V, Dehee A, Chikhi-Brachet R, Piolot T, Coppey-Moisan M, Nicolas JC. Mapping EBNA-1 domains involved in binding to metaphase chromosomes. J Virol 1999;73:4385–92.

21. Ballestas ME, Chatis PA, Kaye KM. Efficient persistence of extrachromosomal KSHV DNA mediated by latency-associated nuclear antigen. Science 1999;284:641–4.

22. Baiker A, Maercker C, Piechaczek C, et al. Mitotic stability of an episomal vector containing a human scaffold/matrix-attached region is provided by association with nuclear matrix. Nat Cell Biol 2000;2:182–4.

23. Ford JH, Schultz CJ, Correll AT. Chromosome elimination in micronuclei: a common cause of hypoploidy. Am J Hum Genet 1988;43:733–40.

24. Nath J, Tucker JD, Hando JC. Y chromosome aneuploidy, micronuclei, kinetochores and aging in men. Chromosoma 1995;103:725–31.

25. Camps J, Ponsa I, Ribas M, et al. Comprehensive measurement of chromosomal instability in cancer cells: combination of fluorescence *in situ* hybridization and cytokinesis-block micronucleus assay. FASEB J 2005;19: 828–30.

26. Shimizu N, Shimura T, Tanaka T. Selective elimination of acentric double minutes from cancer cells through the extrusion of micronuclei. Mutat Res 2000; 448:81–90.

27. Shimizu N, Kamezaki F, Shigematsu S. Tracking of microinjected DNA in live cells reveals the intracellular behavior and elimination of extrachromosomal genetic material. Nucleic Acids Res 2005;33:6296–307.

28. Labidi B, Gregoire M, Frackowiak S, Hernandez VD, Bouteille M. RNA polymerase activity in PtK1 micronuclei containing individual chromosomes. An *in vitro* and *in situ* study. Exp Cell Res 1987;169:233–44.

29. Shimizu N, Itoh N, Utiyama H, Wahl G. Selective entrapment of extrachromosomally amplified DNA by nuclear budding and micronucleation during S-phase. J Cell Biol 1998;140:1307–20.

30. Spicer DB, Sonenshein GE. An antisense promoter of the murine c-myc gene is localized within intron 2. Mol Cell Biol 1992;12:1324–9.

31. Celano P, Berchtold CM, Kizer DL, et al. Characterization of an endogenous RNA transcript with homology to the antisense strand of the human c-myc gene. J Biol Chem 1992;267:15092–6.

32. Shimizu N, Miura Y, Sakamoto Y, Tsutsui K. Plasmids with a mammalian replication origin and a matrix attachment region initiate the event similar to gene amplification. Cancer Res 2001;61:6987–90.

33. Janicki SM, Tsukamoto T, Salghetti SE, et al. From silencing to gene expression: real-time analysis in single cells. Cell 2004;116:683–98.

34. Thompson CB, Challoner PB, Neiman PE, Groudine M. Levels of c-myc oncogene mRNA are invariant throughout the cell cycle. Nature 1985;314: 363–6.

35. Kanda T, Otter M, Wahl GM. Coupling of mitotic chromosome tethering and replication competence in Epstein-Barr virus-based plasmids. Mol Cell Biol 2001; 21:3576–88.

36. Shimizu N, Hashizume T, Shingaki K, Kawamoto JK. Amplification of plasmids containing a mammalian replication initiation region is mediated by controllable conflict between replication and transcription. Cancer Res 2003;63: 5281–90.

37. Shimizu N, Shingaki K, Kaneko-Sasaguri Y, Hashizume T, Kanda T. When, where and how the bridge breaks: anaphase bridge breakage plays a crucial role in gene amplification and HSR generation. Exp Cell Res 2005;302:233–43.